

# Semi-relativistic meson exchange currents in $(e, e')$ and $(e, e'p)$ reactions

J.E. Amaro<sup>1</sup>, M.B. Barbaro<sup>2,3</sup>, J.A. Caballero<sup>3</sup>, F. Kazemi Tabatabaei<sup>1</sup>

<sup>1</sup>*Departamento de Física Moderna, Universidad de Granada, E-18071 Granada, SPAIN*

<sup>2</sup>*Dipartimento di Fisica Teorica, Università di Torino and INFN, Sezione di Torino  
Via P. Giuria 1, 10125 Torino, ITALY*

<sup>3</sup>*Departamento de Física Atómica, Molecular y Nuclear  
Universidad de Sevilla, Apdo. 1065, E-41080 Sevilla, SPAIN*

---

## Abstract

Electron-induced one-nucleon knock-out observables are computed for moderate to high momentum transfer making use of semi-relativistic expressions for the one-body and two-body meson-exchange current matrix elements. Emphasis is placed on the semi-relativistic form of the  $\Delta$ -isobar exchange current and several prescriptions for the dynamical-equivalent form of the  $\Delta$ -propagator are analyzed. To this end, the inclusive transverse response function, evaluated within the context of the semi-relativistic approach and using different prescriptions for the  $\Delta$ -propagator, is compared with the fully relativistic calculation performed within the scheme of the relativistic Fermi gas model. It is found that the best approximation corresponds to using the traditional static  $\Delta$ -propagator. These semi-relativistic approaches, which contain important aspects of relativity, are implemented in a distorted wave analysis of quasielastic  $(e, e'p)$  reactions. Final state interactions are incorporated through a phenomenological optical potential model and relativistic kinematics is assumed when calculating the energy of the ejected nucleon. The results indicate that meson exchange currents may modify substantially the  $TL$  asymmetry for high missing momentum.

*PACS:* 25.30.Fj, 14.20.Gk, 24.10.Jv, 24.10.Eq, 21.60.Cs

*Keywords:* Nuclear reactions, Exclusive electron scattering, Inclusive electron scattering, Meson exchange currents, Relativistic Fermi Gas.

---

# 1 Introduction

Electron induced one-nucleon emission reactions near the quasielastic peak are clearly dominated by one-body (OB) dynamics since such kinematics roughly corresponds to the virtual photon interacting directly with a bound nucleon [1, 2, 3]. Under these conditions it has been possible to analyze a considerable amount of data for a variety of nuclei and to study many aspects of the reaction mechanism. Most of these studies have been based on the standard distorted-wave impulse approximation (DWIA), where the OB current matrix elements are computed using single-particle wave functions obtained as solutions of the Schrödinger equation with phenomenological potentials. Recently [4, 5, 6, 7], efforts have been made to develop a fully relativistic description of the process in order to describe consistently the high momentum and energy transfer region [8]. This constitutes the basis of the relativistic distorted-wave impulse approximation (RDWIA).

Within the scheme of non-relativistic approaches, the role played by correlations beyond the mean field and their impact on the overlap functions and spectroscopic factors has been investigated in several works. Many-body calculations [9, 10] including short-range correlations (SRC) of central type only, have shown a small effect over the quasi-hole overlap functions and, accordingly, over the  $(e, e'p)$  cross section. In [11] the SRC were shown not to modify substantially the mean field  $(e, e'p)$  results at high momentum and low excitation energy. In recent works a significant effort has been made to improve the analysis by including the tensor and spin-isospin channels [12, 13] as well as long-range correlations [14, 15]. It is important to point out that the extraction of spectroscopic factors from the analysis of  $(e, e'p)$  experiments is still not free from ambiguities. This would require an accurate knowledge of the reaction mechanism. In this sense, a RDWIA calculation, compared to DWIA, gives rise to a different quenching of the  $(e, e'p)$  cross section, hence leading to different spectroscopic factors [4] (larger for RDWIA).

The two-body meson exchange currents (MEC) may also play a significant role in the description of electron scattering observables since they are connected to the nuclear correlations by the continuity equation. In fact the interplay between correlations and MEC in  $(e, e'p)$  reactions is far from trivial; rigorously the concept of overlap function is not enough to describe the process in presence of two-body current operators, and therefore the effect of correlations in presence of MEC may be not simply parameterizable by a spectroscopic factor. This idea is supported by calculations of the inclusive transverse response for nuclear matter within the correlated basis function perturbation theory [16], that have shown a significant effect due to MEC, contrary to the much smaller effect usually found for uncorrelated calculations [17]. Before a complete calculation of the exclusive response functions including MEC within a sophisticated correlated model of the reaction be attempted, it is necessary to calibrate different approaches to the calculation in uncorrelated models, as a first step beyond the DWIA.

Thus in this work we restrict our attention to the mean-field (uncorrelated) model and evaluate the role played by the MEC in quasielastic inclusive and exclusive electron scattering reactions. In the case of exclusive  $(e, e'p)$  processes, a theoretical evaluation of MEC, including the usual pion-in-flight (P), contact (C) and Delta-Isobar ( $\Delta$ ), has been presented in refs. [18, 19, 20]. In [20] substantial differences were found with respect to the results

of ref. [19], particularly for the interference  $TL$  response. The analysis in [19], which treats final state interactions (FSI) through a real potential, was extended to higher momentum transfer in refs. [21, 22] where some relativistic corrections were also included in the OB current operator. Instead the standard non-relativistic MEC operators [23, 24] were used except for a modified “dynamical”  $\Delta$ -propagator that depends on the invariant energy  $\sqrt{s}$  of the  $\Delta$ . More recently, the theoretical model of [18] has been refined in [25] modifying also the  $\Delta$ -propagator in order to include the  $\Delta$ -invariant mass. The use of a proper “dynamical” propagator in the  $\Delta$ -current has been discussed at length, concerning mainly the case of two-particle emission reactions [26, 27, 28]. One of the central questions is how to determine  $\sqrt{s}$  in a way that could be easily implemented in existing models for  $(e, e')$  and  $(e, e'p)$  reactions.

In general the appropriate choice of  $\sqrt{s}$  will depend on the specific dynamical model for the reaction mechanism. Hence a proper description of the reaction dynamics through an adequate choice of the currents and kinematics results necessary. For high momentum transfer relativistic effects play a significant role and therefore relativity should enter in the description of kinematics and/or current matrix elements. Within a fully relativistic model, MEC effects in  $(e, e'p)$  have been computed recently in [29], where only the contact (or “seagull”) current has been considered. Due to the complexity of the fully relativistic two-body currents, particularly the  $\Delta$  one, in this work we start by developing reasonable semi-relativistic expressions for all the two-body currents (P, C and  $\Delta$ ) that can be easily implemented in existing non-relativistic descriptions of the reaction mechanism. These semi-relativistic currents retain important aspects of relativity and hence they may be used to describe properly recent experiments performed at high momentum and energy transfers.

In this paper we discuss the one-particle emission sector, introducing a new semi-relativistic (SR) approximation for the three MEC operators which, in conjunction with the SR form of the OB current derived in [30] (see [31] for a recent review on these expansions), makes it possible to evaluate quasielastic  $(e, e')$  and  $(e, e'p)$  observables. The SR currents are obtained by a direct Pauli reduction of the corresponding relativistic currents in powers only of  $p/m_N$ , being  $p$  the initial momentum (missing momentum) of the bound nucleon and  $m_N$  the nucleon mass. The transfer momentum  $q$  and transfer energy  $\omega$  are treated exactly. The SR form of the OB current operator was checked in [30] where, assuming relativistic kinematics, the inclusive nuclear electroweak responses were found to agree with the exact relativistic Fermi gas (RFG) results within a few percent. This SR-OB expression was also used for inclusive  $(e, e')$  processes with polarized nuclei [32], and for coincidence  $(e, e'p)$  calculations with unpolarized [6, 10] and polarized [33, 34, 35] targets. The SR expressions for the MEC operators were obtained in [36] in the case of the pionic and contact currents. In [31, 37] a comparison between the SR-MEC predictions for the inclusive transverse response and the exact RFG results is presented.

One of the goals of this work is to derive a semi-relativistic expression for the  $\Delta$ -exchange current and compare its prediction for the inclusive transverse response function with the exact relativistic result obtained within the RFG model of ref. [38]. This comparison, carried out in the inclusive channel (section 2), makes it possible to test the reliability of the different prescriptions of the “dynamical”  $\Delta$ -propagator to be used in exclusive  $(e, e'p)$  processes (section 3). Once this is settled, the impact of the relativistic MEC over the exclusive

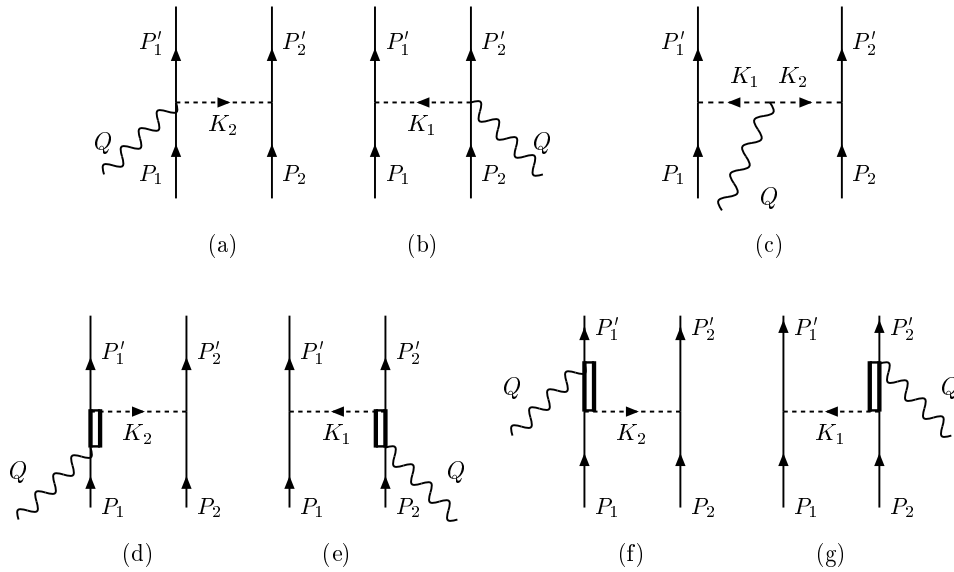


Figure 1: Feynman diagrams contributing to the two-body current with one pion-exchange. Contact (C) (a,b), pionic (P) (c), and isobar ( $\Delta$ ) (d)–(g) are included in this work.

response functions is evaluated for moderate to high momentum transfer. Finally, in section 4 we draw our conclusions.

## 2 Inclusive transverse response

The impact of meson exchange currents on inclusive electron scattering has been traditionally investigated in a non-relativistic framework and relativistic corrections have been implemented making use of a power expansion in the momenta of the nucleons and of the exchanged photon [39, 40, 41]. In refs. [31, 38] a semi-relativistic analysis of the MEC (P, S and  $\Delta$ ) currents, represented in fig. 1, has been performed in the context of the RFG with the aim of finding simple prescriptions for implementing relativistic effects into non-relativistic calculations. Within the RFG model, it is possible to perform a fully relativistic calculation of the inclusive response functions, using exact relativistic kinematics, currents and propagators. Hence the inclusive transverse response function of nuclear matter can be used to test the quality of the semi-relativistic MEC, to be applied in the next section to semi-inclusive processes.

In this section we focus on the  $\Delta$  current, represented by diagrams (d)–(g) of fig. 1, putting emphasis on the “dynamical” treatment of the  $\Delta$  propagator, an aspect of the problem which was neglected in the SR model of [38]. Restricting our attention to the case of one-particle emission processes, the contribution of the  $\Delta$  current to the transverse nuclear response

function is obtained as the interference between the  $\Delta$  and the OB currents. In the Fermi gas model it reads

$$R_{\Delta\text{-OB}}^T(q, \omega) = \frac{3Z}{8\pi k_F^3} 2\text{Re} \int_{h < k_F} d^3h \delta(E_{\mathbf{p}} - E_{\mathbf{h}} - \omega) \mathcal{N}_{\mathbf{ph}} \text{Tr} \left[ \mathbf{j}_T^{OB}(\mathbf{p}, \mathbf{h})^* \cdot \mathbf{j}_T^{\Delta}(\mathbf{p}, \mathbf{h}) \right], \quad (1)$$

where  $\mathbf{p} = \mathbf{h} + \mathbf{q}$  is the momentum of the ejected particle,  $\mathbf{j}_T$  is the transverse (perpendicular to  $\mathbf{q}$ ) component of  $\mathbf{j}$  and  $k_F$  is the Fermi momentum. In the RFG model  $E_{\mathbf{k}} = \sqrt{\mathbf{k}^2 + m_N^2}$ , whereas in the non-relativistic (NR) Fermi gas,  $E_{\mathbf{k}} = m_N + \epsilon_{\mathbf{k}} = m_N + \mathbf{k}^2/(2m_N)$ . Moreover, the factor  $\mathcal{N}_{\mathbf{ph}}$ , arising from the spinor normalization, is  $m_N^2/(E_{\mathbf{p}}E_{\mathbf{h}})$  for RFG and 1 in a NR model. The particle-hole functions  $\mathbf{j}_T^a(\mathbf{p}, \mathbf{h})$  (which implicitly include spin and isospin indices) for the OB or  $\Delta$  currents are obtained from the matrix elements of the corresponding operator between the ground state  $C$  and the p-h excited state according to:

$$\langle p, h^{-1} | \mathbf{j}^a(Q) | C \rangle = (2\pi)^3 \delta^3(\mathbf{q} + \mathbf{h} - \mathbf{p}) \mathcal{N}_{\mathbf{ph}} \mathbf{j}^a(\mathbf{p}, \mathbf{h}). \quad (2)$$

The non relativistic two-body  $\Delta$  current used in this paper has been obtained from the relativistic one in the limit of small momenta by following the procedure sketched in ref. [38]; it can be written in momentum space as

$$\begin{aligned} & \mathbf{j}_{nr}^{\Delta}(\mathbf{p}'_1, \mathbf{p}'_2, \mathbf{p}_1, \mathbf{p}_2) \\ &= \frac{1}{9} \frac{G_1}{2m_N} \frac{f_{\pi N\Delta}}{m_{\pi}} \frac{f}{m_{\pi}} \left\{ G_{\Delta}(P_1 + Q) \mathbf{q} \times \left[ -\mathbf{k}_2 \times \boldsymbol{\sigma}^{(1)} + 2i\mathbf{k}_2 \right] \left[ 2\tau_3^{(2)} - i[\boldsymbol{\tau}^{(1)} \times \boldsymbol{\tau}^{(2)}]_z \right] \right. \\ & \quad \left. + G_{\Delta}(P_1 - Q) \mathbf{q} \times \left[ \mathbf{k}_2 \times \boldsymbol{\sigma}^{(1)} + 2i\mathbf{k}_2 \right] \left[ 2\tau_3^{(2)} + i[\boldsymbol{\tau}^{(1)} \times \boldsymbol{\tau}^{(2)}]_z \right] \right\} \frac{\mathbf{k}_2 \cdot \boldsymbol{\sigma}^{(2)}}{\mathbf{k}_2^2 + m_{\pi}^2} \\ & \quad + (1 \longleftrightarrow 2), \end{aligned} \quad (3)$$

where  $P_i, P'_i$  are the four-momenta of the initial and final nucleons defined in fig. 1,  $\mathbf{k}_i = \mathbf{p}'_i - \mathbf{p}_i$  is the momentum transferred to the  $i$ -th nucleon and  $G_{\Delta}(P)$  is the non-relativistic (dynamical)  $\Delta$  propagator, which will be later discussed in detail. We use the following values for the coupling constants:  $G_1 = 4.2$ ,  $f^2/4\pi = 0.079$ ,  $f_{\pi N\Delta} = 2.24$ .

The MEC ph matrix elements are obtained by summing over all the single-particle states occupied in the ground-state Slater determinant:

$$\langle p, h^{-1} | \mathbf{j}_{MEC}(Q) | C \rangle = \sum_{k < F} [\langle pk | \mathbf{j}_{MEC}(Q) | hk \rangle - \langle pk | \mathbf{j}_{MEC}(Q) | kh \rangle], \quad (4)$$

where the sum implicitly includes spin and isospin indices. In the case of nuclear matter only the exchange term, represented by the many-body diagrams of fig. 2, survives, due to spin and isospin symmetries. Moreover, it can be proved that the exchange  $\Delta$  terms represented by diagrams (f) and (g) are also zero in nuclear matter. In the case of finite nuclei there exists however a contribution coming from the direct  $\Delta$  term, which, although small, has been included in the calculations presented in next section.

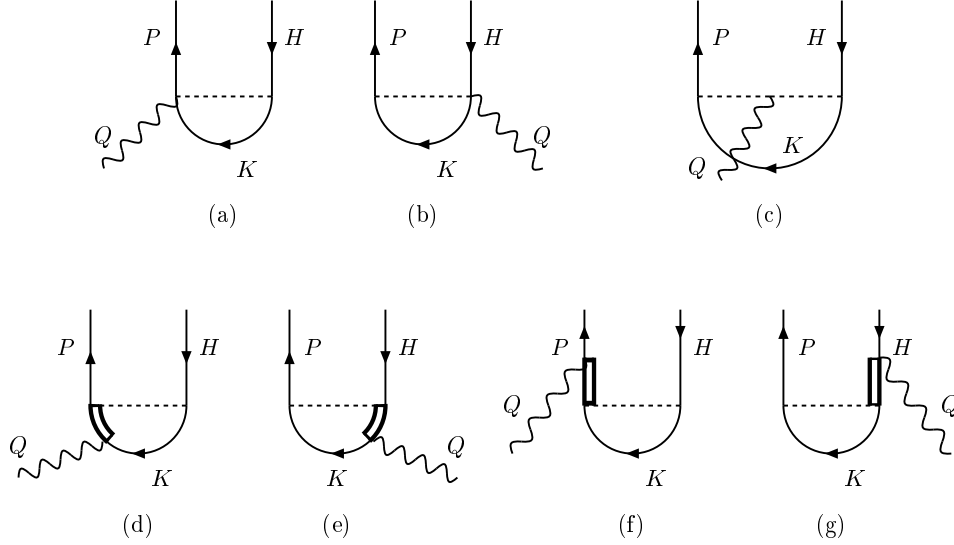


Figure 2: Exchange MEC diagrams contributing to the one-particle emission responses computed in this work. In the vertex-type isobar diagrams (d,e) different prescriptions for the dynamical  $\Delta$  propagator are discussed in the text.

Using eqs. (3,4) the particle-hole matrix element of the non-relativistic  $\Delta$  current in nuclear matter results

$$\mathbf{j}_{nr}^{\Delta}(\mathbf{p}, \mathbf{h}) = -i\delta_{t_p t_h} \tau_h \frac{4}{9} \frac{G_1}{2m_N} \frac{f_{\pi N \Delta}}{m_{\pi}} \frac{f}{m_{\pi}} \int \frac{d^3 k}{(2\pi)^3} \theta(k_F - k) \times \left\{ G_{\Delta}(\mathbf{k} + \mathbf{q}) \mathbf{B}(\mathbf{h} - \mathbf{k})_{s_p s_h} + G_{\Delta}(\mathbf{k} - \mathbf{q}) \mathbf{B}(\mathbf{p} - \mathbf{k})_{s_p s_h} \right\}, \quad (5)$$

where  $\tau_h = 1$  if  $h$  is a proton and  $-1$  if neutron, and we have defined the function

$$\mathbf{B}(\mathbf{p} - \mathbf{k})_{ss'} = \frac{[\boldsymbol{\sigma}_{ss'} \cdot (\mathbf{p} - \mathbf{k})](\mathbf{p} - \mathbf{k}) + (\mathbf{p} - \mathbf{k})^2 \boldsymbol{\sigma}_{ss'}}{(\mathbf{p} - \mathbf{k})^2 + m_{\pi}^2}. \quad (6)$$

If the  $\mathbf{k}$ -dependence of the  $\Delta$ -propagator is neglected, then the integral in eq. (5) can be solved analytically<sup>1</sup> (see ref. [17] for its explicit form).

The relativistic expression for the currents can be found in [38] and yields results which differ significantly from the non-relativistic ones even if the momentum transfer is as low as 500 MeV/c. This difference is due in part to the relativistic kinematics (RK), which can be easily implemented in the NR model by the replacement

$$p = \sqrt{2m_N(\epsilon_{\mathbf{h}} + \omega)} \rightarrow \sqrt{E_{\mathbf{p}}^2 - m_N^2} \simeq \sqrt{2m_N \left[ \epsilon_{\mathbf{h}} + \omega \left( 1 + \frac{\omega}{2m_N} \right) \right]} \quad (7)$$

<sup>1</sup>Note that in this section we are not including  $\pi N$  form factors in order to obtain an analytical result for numerical convenience. In the next section they will be properly included.

in the non-relativistic response. The above prescription amounts to a shift of the transferred energy in the response functions, with the exception of the electromagnetic form factors, that must be computed for the unshifted value of  $\omega$ . Moreover, the NR results can be brought closer to the relativistic ones if the SR form of the current operators

$$\mathbf{j}_{T,SR}^a(\mathbf{p}, \mathbf{h}) \equiv \frac{1}{\sqrt{1+\tau}} \mathbf{j}_{T,nr}^a(\mathbf{p}, \mathbf{h}) \quad (8)$$

is employed for  $a = \text{OB, C, P, } \Delta$ .

The result shown in eq. (8) has been obtained (see refs. [31, 36, 38] for details) by a direct Pauli reduction expanding in powers of  $\mathbf{h}/m_N$  to first order in the case of the OB current [30], and to leading order in the MEC pionic and contact cases [36] though a more complex structure was found for the seagull current, for which the approximate factorized form (8) was introduced and tested in [37]. In this paper we use a similar 'factorized' expression for the SR  $\Delta$ -current that was already proposed in [38]. The  $\tau$ -dependent factor ( $\tau = |Q^2|/4m_N^2$ ) in eq. (8) arises from the spinology and produces a reduction of the responses.

Let us now discuss the  $\Delta$  propagator  $G^\Delta$ , appearing in the  $\Delta$  current, eqs. (3,5). In a fully relativistic theory,  $G^\Delta$  is given by the Rarita-Schwinger tensor

$$G_{\beta\rho}^\Delta(P) = -\frac{P + m_\Delta}{P^2 - m_\Delta^2} \left[ g_{\beta\rho} - \frac{1}{3} \gamma_\beta \gamma_\rho - \frac{2}{3} \frac{P_\beta P_\rho}{m_\Delta^2} - \frac{1}{3} \frac{\gamma_\beta P_\rho - \gamma_\rho P_\beta}{m_\Delta} \right], \quad (9)$$

where  $m_\Delta$  is the  $\Delta$  mass. The possible decay of the isobar into a  $N\pi$  state is accounted for by the substitution  $m_\Delta \rightarrow m_\Delta - \frac{i}{2}\Gamma(P^2)$  in the denominator, where the function  $\Gamma(P^2)$  is the width of the resonance (see [42, 43]).

The non-relativistic version of this propagator is defined by the positive energy sector of eq. (9) for spatial indices and small momenta [38]

$$G_{ij}^\Delta(P) \simeq \frac{P + m_\Delta}{P^2 - m_\Delta^2} \left( \delta_{ij} + \frac{1}{3} \gamma_i \gamma_j \right) \longrightarrow G_\Delta(P) \left( \frac{2}{3} \delta_{ij} - \frac{i}{3} \epsilon_{ijk} \sigma_k \right). \quad (10)$$

Note that diagrams (d–g) of fig. 1 correspond to different momenta in the propagators, namely  $G_\Delta(P_1 + Q)$  and  $G_\Delta(P'_1 - Q)$ : these, referred to as  $\Delta$ -excitation ( $G_\Delta^I$ ) and  $\Delta$ -deexcitation ( $G_\Delta^{II}$ ) in [21, 25], denote the propagator for a  $\Delta$  created after and before photo-absorption, respectively.

The static limit approximation to  $G^\Delta$  consists in taking

$$\frac{P + m_\Delta}{P^2 - m_\Delta^2} \simeq \frac{m_N \gamma_0 + m_\Delta}{P^2 - m_\Delta^2} \rightarrow \frac{m_N + m_\Delta}{m_N^2 - m_\Delta^2} = \frac{1}{m_N - m_\Delta}, \quad (11)$$

where we have used  $P^2 \simeq m_N^2$  for  $P = P_1 + Q$  or  $P = P'_1 - Q$  and  $q, \omega$  small, since  $P_1$  and  $P'_1$  are the four-momenta of the initial and final nucleons. In this case, the two propagators are equal, i.e.,  $G_\Delta(P_1 + Q) = G_\Delta(P'_1 - Q) = (m_N - m_\Delta)^{-1}$  and can be factorized out in eq. (3), thus yielding the traditional form of the non-relativistic current [17, 23].

The effects introduced by relativity can be appreciated in fig. 3. Here we show the inclusive transverse response for two values of the momentum transfer,  $q = 0.5 \text{ GeV}/c$  (top panel) and  $q = 1 \text{ GeV}/c$  (bottom panel). The fully relativistic calculation performed within the

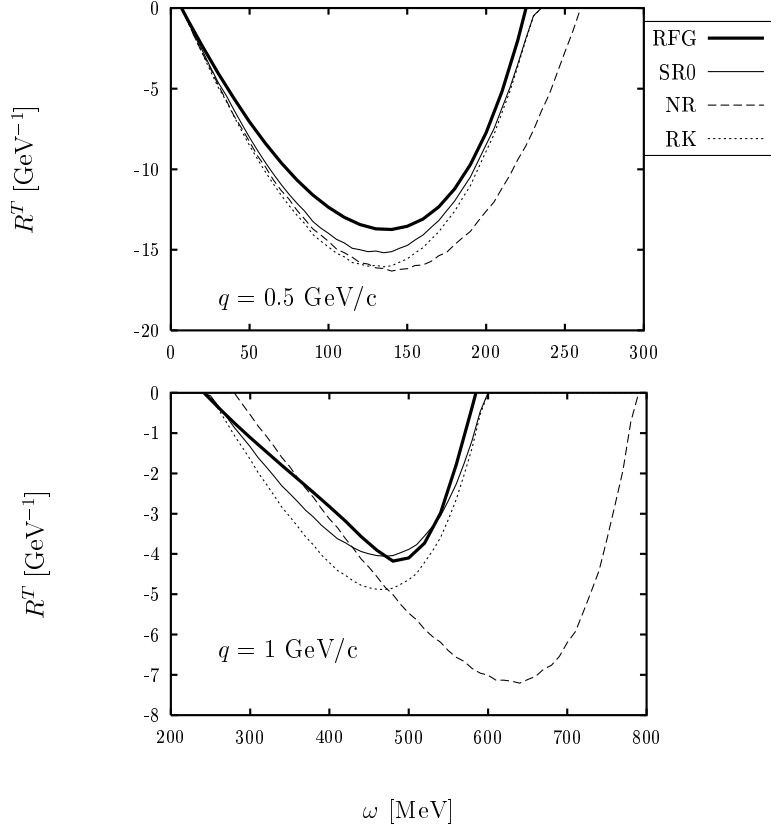


Figure 3: Contribution of the  $\Delta$  to the transverse response function for  $q = 500$  and  $1000$  MeV/c. The results corresponding to the relativistic Fermi gas (RFG) are compared with the non-relativistic (NR) Fermi gas, including relativistic kinematic (RK), and using the semi-relativistic (SR0) approach for the electromagnetic currents.

RFG model of ref. [38] (thick solid line) is compared with various non-relativistic approaches: the traditional non-relativistic model (NR), the NR model but including relativistic kinematics (denoted as RK), and the results corresponding to the semi-relativistic currents, using in addition relativistic kinematics (denoted as SR0). Apart from the RFG, where the Rarita-Schwinger propagator is used including the  $\Delta$  width, the other results have been evaluated employing the static limit approximation for the  $\Delta$  propagator, for which  $\sqrt{s} = m_N$ , and therefore  $\Gamma_\Delta(s) = 0$ , since  $s$  is below the threshold,  $m_N + m_\pi$ . Note the crucial role played by the relativistic kinematics and, moreover, how the SR approach, compared to the RK case, improves the agreement with the RFG results.

Next we study the effect of including a “dynamical”  $\Delta$  propagator within the SR model. This can be done by using different approximations for the propagators,  $G_\Delta(K + Q)$  and  $G_\Delta(K - Q)$ , appearing in the non-relativistic current, eq. (5), under the requirement that the new “dynamical” propagator be independent of  $\mathbf{k}$ : only in this case it can be easily introduced into non-relativistic calculations.

The results for the  $\Delta$ -OB transverse response computed within the SR model, and using different prescriptions for the  $\Delta$  propagator, are displayed in fig. 4. As in the previous figure and for comparison, we present the fully relativistic results (RFG) and the SR approach using the static limit for the  $\Delta$  propagator (SR0). In all the cases, relativistic kinematics is assumed. The various approaches considered to describe the “dynamical”  $\Delta$  propagator are below listed and discussed in some detail.

- 1) The propagator is written, as suggested in refs. [26, 28], as

$$G_{\Delta}(P) = \frac{1}{\sqrt{s} - m_{\Delta} + \frac{i}{2}\Gamma_{\Delta}(s)}, \quad (12)$$

where  $s = P^2$  and  $\sqrt{s}$  is the available energy in the  $\Delta$  rest system. The approximate values of  $s$  are obtained by neglecting the momentum  $k$  and kinetic energy  $\epsilon_{\mathbf{k}}$  compared with  $q$  and the nucleon mass  $m_N$ , i.e.,

$$s^I \equiv (K + Q)^2 = (E_{\mathbf{k}} + \omega)^2 - (\mathbf{k} + \mathbf{q})^2 \simeq (m_N + \omega)^2 - q^2 \quad (13)$$

$$s^{II} \equiv (K - Q)^2 \simeq (m_N - \omega)^2 - q^2. \quad (14)$$

As we observe in fig. 4, this prescription (denoted as SR1) produces a hardening of the response function, that is more pronounced for high  $q$ , and under-estimates the exact result at the peak.

- 2) This second prescription is obtained, as suggested in refs. [25, 28], by using the static approximation in the de-excitation diagram, fig. 2e, i.e.,  $s^{II} \simeq m_N^2$ , and a dynamical propagator in the  $\Delta$  excitation diagram, fig. 2d. In this case we use the same value  $s^I$  as in eq. (13). As shown in fig. 4, this prescription (labelled as SR2) still produces a hardening of the response, but now the response function is larger than the relativistic one. We note also that the SR2 curve crosses the static SR0 result precisely at the position of the quasielastic peak (QEP). In fact, this is determined by  $(m_N + \omega)^2 - q^2 = m_N^2$ , hence eq. (13) gives the static result,  $\sqrt{s^I} = m_N$ .

- 3) From eq. (10) we may write

$$\frac{P + m_{\Delta}}{P^2 - m_{\Delta}^2} \simeq \frac{E\gamma_0 - \mathbf{q} \cdot \boldsymbol{\gamma} + m_{\Delta}}{\sqrt{s} + m_{\Delta}} \frac{1}{\sqrt{s} - m_{\Delta}} \quad (15)$$

for  $P = K + Q$ . The result given by eq. (12) is re-obtained when the first term in the right hand side of eq. (15) is close to one. Note that for  $q$  large,  $\sqrt{s}$  can be significantly different from  $E$ , while one cannot neglect the term  $\mathbf{q} \cdot \boldsymbol{\gamma}$ . This would give an additional spin-dependent term and the propagator would get tangled. Instead, a possible way to proceed is by taking partially into account the  $q$ -dependence in the numerator in the way:

$$G_{\Delta}(K + Q) \simeq \frac{m_N + \omega + q + m_{\Delta}}{\sqrt{s^I} + m_{\Delta}} \frac{1}{\sqrt{s^I} - m_{\Delta}} \quad (16)$$

$$G_{\Delta}(K - Q) \simeq \frac{m_N + \omega - q + m_{\Delta}}{\sqrt{s^{II}} + m_{\Delta}} \frac{1}{\sqrt{s^{II}} - m_{\Delta}}, \quad (17)$$

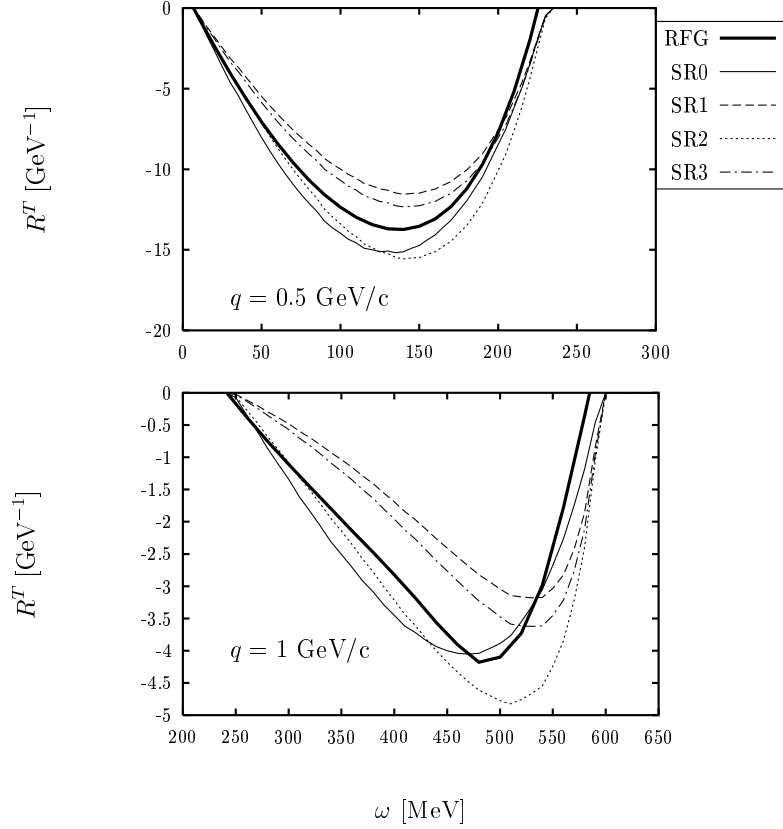


Figure 4: Contribution of the  $\Delta$  to the transverse response function. using different prescriptions for the  $\Delta$  propagator, discussed in the text

where  $s^{I,II}$  are given in eqs. (13,14). This procedure allows us to write down an approximate diagonal expression for the  $\Delta$  propagator, and the corresponding results are denoted in fig. 4 as SR3. The reduction of the response function is shown not to be as large as in the SR1 case.

Summarizing, from fig. 4 we may conclude that none of the above approximations proposed for the dynamical  $\Delta$  propagator is entirely satisfactory. In fact we observe that the best result, compared with the fully relativistic RFG one, corresponds to the static limit approximation.

To complete this discussion, we note that the role of the width  $\Gamma$  in the SR models of fig. 4 is irrelevant since the approximate values taken for  $\sqrt{s}$  are far below the pole for these kinematics. In fact, for the prescription SR1 we have from eq. (13):

$$\omega = \sqrt{s^I + q^2} - m_N. \quad (18)$$

This means that for  $q = 1$  GeV/c and  $\sqrt{s^I} = m_\Delta$ , we get  $\omega \sim 649$  MeV, which is well above the allowed region of the QEP, while the threshold,  $\sqrt{s^I} = m_N + m_\pi$ , is reached for  $\omega \sim 531$

MeV, below which the  $\Delta$  width is zero. Hence only the small tail of the  $\Delta$  close to the threshold is being considered in this region of energy.

Actually in the relativistic model things are totally different because the pole is reached inside the allowed energy region. Indeed the delicate energy balance in the denominator makes the value of the inner momentum  $\mathbf{k}$  to play a role. Instead of (18) a better approximation to the exact relation is represented by

$$\omega = \sqrt{s^I + (\mathbf{q} + \mathbf{k})^2} - m_N . \quad (19)$$

In this case the pole is first reached at

$$\omega = \sqrt{m_\Delta^2 + (q - k_F)^2} - m_N , \quad (20)$$

which gives  $\omega \sim 511$  MeV, close to the peak for  $q = 1$  GeV/c.

Thus we have considered two new prescriptions, denoted as SR4 and SR5. To help the reader they are shown in a separate figure (fig. 5), where they are again compared with the fully relativistic calculation (RFG) and the static limit approach (SR0). These new prescriptions are based on the value assigned to  $\sqrt{s}$ , such that the position of the pole be closer to the relativistic case. More precisely:

- 4) One considers  $\sqrt{s^I} = \sqrt{s_{NN}} - m_N$ , being  $s_{NN}$  the invariant energy of the two outgoing nucleons, suggested in [26, 28] for two-nucleon knock-out, and apparently applied also to one-nucleon emission in [25]. The meaning of  $s_{NN}$  for this case is doubtful, since there is only one particle in the final state. However, from the  $\Delta$ -excitation diagram, fig. 2d, we see that  $\mathbf{k}, \mathbf{h}$  are two entering momenta and  $\mathbf{p}, \mathbf{k}$  the two exiting ones. Hence the prescription SR4 in fig. 5 is based on the approximation:

$$s_{NN} \simeq (P + K)^2 = (E_{\mathbf{h}} + E_{\mathbf{k}} + \omega)^2 - (\mathbf{h} + \mathbf{k} + \mathbf{q})^2 \simeq (2m_N + \omega)^2 - q^2 . \quad (21)$$

In this case the pole for  $q = 1$  GeV/c is reached at  $\omega \simeq 513$  MeV, inside the QE region. However, from the results in fig. 5, this prescription appears to be less satisfactory than the previous ones.

- 5) Finally, the prescription SR5 is obtained by exploiting eq. (20) that gives the right position at which the pole is first reached and defining

$$s^I = (m_N + \omega)^2 - (q - k_F)^2 \quad (22)$$

$$s^{II} = (m_N - \omega)^2 - (q - k_F)^2 . \quad (23)$$

The results show that for  $q = 1$  GeV/c the pole is reached at the right position close to the peak of the response. The change of sign of the response is a consequence of the change of sign of the  $\Delta$  propagator when one crosses the pole.

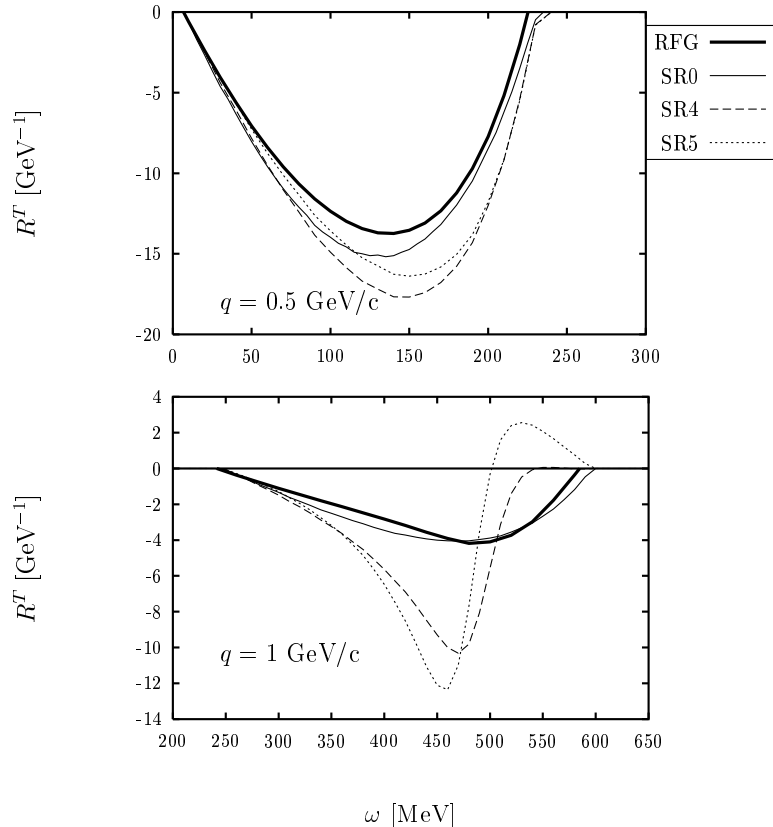


Figure 5: Contribution of the  $\Delta$  to the transverse response function using different prescriptions for the  $\Delta$  propagator discussed in the text.

From fig. 5 we observe that it is not possible to recover the exact relativistic result by using a  $\Delta$  propagator independent of  $\mathbf{k}$ , even if it reaches the pole (in absence, of course, of the  $\Delta$  width) inside the allowed region. In fact the present singularity can only be smoothed, even in the presence of the  $\Delta$  width, after an integration over  $\mathbf{k}$  is performed, as in the relativistic model.

In general we conclude that, if a dynamical propagator has to be used, like in the semi-relativistic approaches discussed here, a smoothed form not hitting the pole is needed in order not to deviate too much from the exact result for the response function. Among the prescriptions analyzed in this section, the static form of the  $\Delta$  propagator produces, in spite of its simplicity, the best agreement with the RFG results in the case of one-particle knockout sector, once relativistic kinematics and semi-relativistic corrections of the currents are used. Therefore, a procedure to “dynamize” the  $\Delta$  propagator as the ones presented here, and its use within the context of a non-relativistic or semi-relativistic distorted wave analysis of quasielastic ( $e, e'$ ) and ( $e, e'p$ ) reactions appears not to give better results than the static approximation. Obviously, this conclusion does not affect the validity of the approximations discussed in [28] for the two-particle emission channel, where the kinematical conditions are

completely different.

In the next section we apply the present semi-relativistic model of MEC to the exclusive ( $e, e'p$ ) response functions of nuclei.

### 3 Exclusive ( $e, e'p$ ) observables

In this section we compute the quasielastic ( $e, e'p$ ) response functions for intermediate to high momentum transfer values within the context of the SR approach introduced in the previous section. As shown in the case of quasielastic inclusive ( $e, e'$ ) responses [30, 31, 37, 38], accounting for relativistic effects requires at least to treat properly the kinematics and relativistic factors in the currents. Referring to the  $\Delta$  current, we make use of the static limit approach for the  $\Delta$  propagator, as this gives rise to the best agreement with the fully-relativistic calculation in the inclusive channel, as shown in the previous Section. As a complete relativistic analysis of all the MEC (P, C and  $\Delta$ ) currents in ( $e, e'p$ ) processes is still lacking, the use of “dynamized”  $\Delta$  propagators within existing NR or SR descriptions of the reaction mechanism does not appear to be well founded and, moreover, these may lead to large discrepancies with the exact calculation.

The general formalism for ( $e, e'p$ ) reactions has been presented in detail in refs. [2, 3, 4, 44] and we refer to them for specifics on the kinematics. Assuming plane waves for the incoming and outgoing electron (treated in the extreme relativistic limit) and parity conservation, the exclusive cross section can be written in the form

$$\frac{d^5\sigma}{d\epsilon' d\Omega'_e d\Omega_{p'}} = K \sigma_M \left( v_L W^L + v_T W^T + v_{TL} W^{TL} \cos \phi' + v_{TT} W^{TT} \cos 2\phi' \right), \quad (24)$$

where  $\epsilon'$  and  $\Omega'_e$  are the energy and solid angle corresponding to the scattered electron and  $\Omega_{p'} = (\theta', \phi')$  is the solid angle for the ejected proton with four-momentum  $P'^\mu = (E', \mathbf{p}')$ . In eq. (24)  $K = p' m_N / (2\pi\hbar)^3$  and  $\sigma_M$  is the Mott cross section. Finally,  $v_\alpha$  are the electron kinematical factors given in refs. [32, 44]. The labels  $L$  and  $T$  refer to the longitudinal and transverse projections of the current matrix elements with respect to the virtual photon direction, respectively.

The hadronic content of the problem enters via the response functions  $W^\alpha$ , which are obtained by taking the appropriate components of the hadronic tensor

$$W^{\mu\nu} = \frac{1}{K} \sum_{m_s M_\alpha} \langle \mathbf{p}' m_s, \Phi_\alpha^{(A-1)} | \hat{J}^\mu(Q) | \Phi_0^{(A)} \rangle^* \langle \mathbf{p}' m_s, \Phi_\alpha^{(A-1)} | \hat{J}^\nu(Q) | \Phi_0^{(A)} \rangle, \quad (25)$$

where a sum over undetected final polarization states is performed. In eq. (25),  $\hat{J}^\mu(Q)$  is the nuclear current operator and we assume the initial state  $|\Phi_0^{(A)}\rangle$  to correspond to a spin-zero nuclear target in its ground state with energy  $E_0^{(A)}$ . The final state  $|\mathbf{p}' m_s, \Phi_\alpha^{(A-1)}\rangle$  is assumed to behave asymptotically as a knockout nucleon with momentum  $\mathbf{p}'$  and spin quantum number  $m_s$  and a residual nucleus left in a bound state, i.e.,  $|\Phi_\alpha^{(A-1)}\rangle = |J_\alpha, M_\alpha\rangle$ , with energy  $E_\alpha^{(A-1)}$ .

In the present distorted wave analysis of ( $e, e'p$ ) reactions, the outgoing nucleon state is described by a wave function solution of the Schrödinger equation with an optical potential

$V_{opt}$  fitted to elastic nucleon-nucleus scattering data. The matrix elements of the hadronic tensor are computed by performing a multipole expansion of both the distorted nucleon wave and the current operators in terms of the usual Coulomb  $C_J$ , electric  $E_J$  and magnetic  $M_J$  multipoles (see refs. [10, 32, 33] for details on the model, and [17, 24, 32] for explicit expressions of the multipole matrix elements of the currents).

To illustrate the role of the relativistic corrections we display in fig. 6 the four unpolarized exclusive response functions for proton knock-out from the  $1p_{1/2}$ -shell in  $^{16}\text{O}$  leading to the residual nucleus  $^{15}\text{N}$ . The kinematics selected corresponds to  $(q, \omega)$ -constant kinematics (sometimes also referred to as quasi-perpendicular kinematics) and the values  $q = 460$  MeV/c and  $q = 995$  MeV/c have been chosen. In each case the value selected of the transferred energy  $\omega$  almost corresponds to the quasi-elastic peak value, i.e.,  $\omega = 100$  MeV and 426 MeV, respectively. FSI are taken into account for  $q = 460$  MeV/c through the optical potential of Comfort and Karp [45], which is appropriate for proton kinetic energies below 183 MeV. In the case of  $q = 995$  MeV/c, as the proton kinetic energy is of the order of  $\sim 430$  MeV, we use instead a Schrödinger-equivalent form of the relativistic global optical potential of ref. [46]. Thus the non-relativistic wave functions correspond to the upper components of the relativistic ones, containing the Darwin term. Results obtained within this approach were compared with a fully relativistic calculation in the impulse approximation [6], i.e., without including the effects of MEC.

In each panel of fig. 6 we compare the results corresponding to the traditional non-relativistic model with non-relativistic kinematics (denoted by NR), including relativistic kinematics (RK), and finally, the semi-relativistic approach discussed in the previous section (SR). All the calculations include MEC. From these results it emerges that, particularly for high  $q$ , the relativistic kinematics plays a crucial role in describing properly the form of the momentum distribution. Note that the allowable missing momentum values are determined by the relation  $|p' - q| \leq p \leq p' + q$ , with  $p'$  fixed by energy conservation. Assuming non-relativistic kinematics the value of  $p'$  is given by

$$p' = \sqrt{2m_N(\epsilon_{\mathbf{h}} + \omega)}, \quad (26)$$

while for relativistic kinematics it results

$$p' = \sqrt{(m_N + \epsilon_{\mathbf{h}} + \omega)^2 - m_N^2} = \sqrt{2m_N(\epsilon_{\mathbf{h}} + \omega) \left(1 + \frac{\epsilon_{\mathbf{h}} + \omega}{2m_N}\right)}. \quad (27)$$

In eqs. (26,27), the energy  $\epsilon_{\mathbf{h}}$  represents the (negative) energy of the bound nucleon. Hence in the case of RK we solve the Schrödinger equation with equivalent energy  $(\epsilon_{\mathbf{h}} + \omega) \left(1 + \frac{\epsilon_{\mathbf{h}} + \omega}{2m_N}\right)$  for the ejected proton instead of the NR energy  $\epsilon_{\mathbf{h}} + \omega$ .

Once relativistic kinematics is selected, the use of SR currents produces an enhancement of the  $L$  and  $TL$  responses and a reduction of the  $T$  and  $TT$  ones, whose magnitude increases with  $q$ . These effects are connected with the factors  $\frac{\kappa}{\sqrt{\tau}} > 1$  and  $\frac{\sqrt{\tau}}{\kappa} \simeq \frac{1}{1+\tau}$  that enter in the SR expressions of the longitudinal and transverse currents, respectively [31, 37]. It is important to point out the particularly large relativistic enhancement observed for the interference  $TL$  response. This is connected to the spin-orbit term [32] contained in the SR charge density but neglected within the NR approach. As shown in [32], the interference

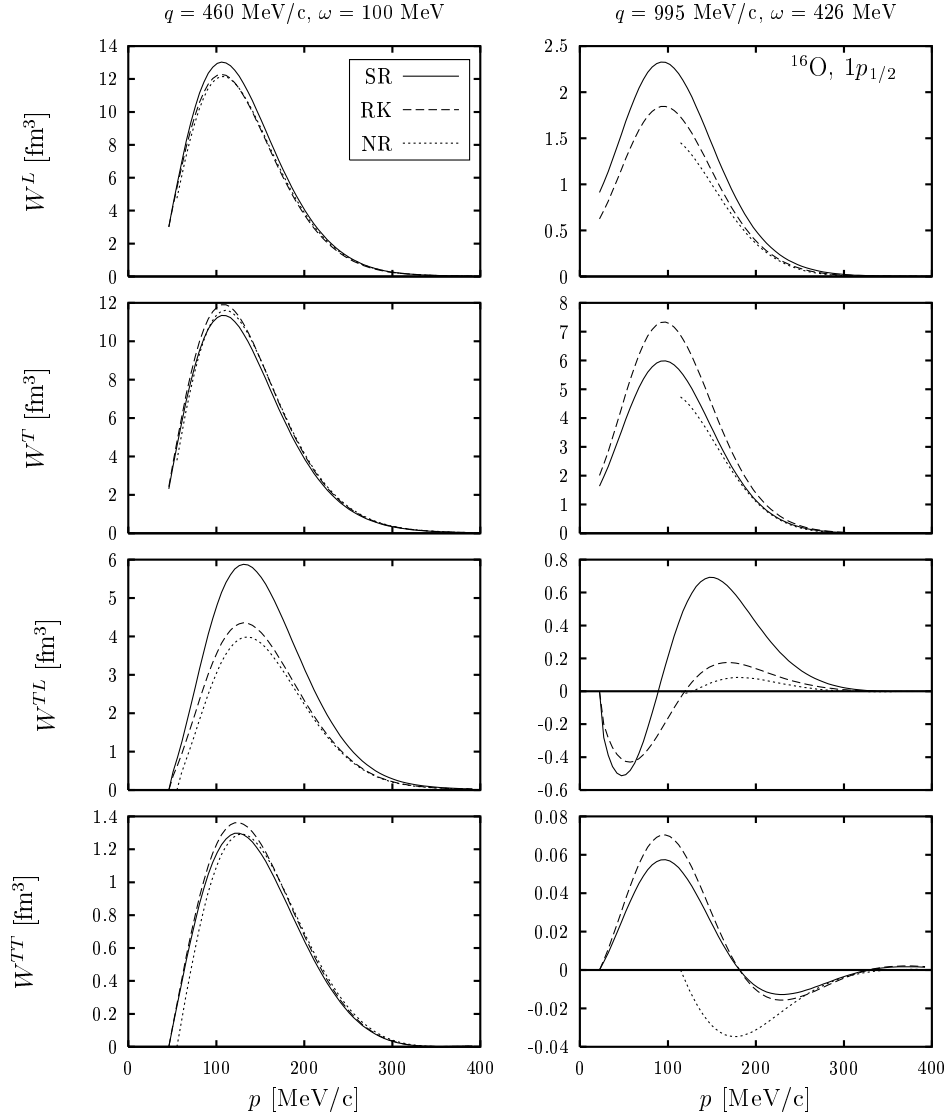


Figure 6: Exclusive response functions for proton knock-out from the  $1p_{1/2}$ -shell in  $^{16}\text{O}$ . Two  $(q, \omega)$ -constant kinematical situations are selected. The traditional non-relativistic results (NR) are compared with the responses obtained including relativistic kinematics (RK) and using the semi-relativistic (SR) form of the currents. All the curves include MEC.

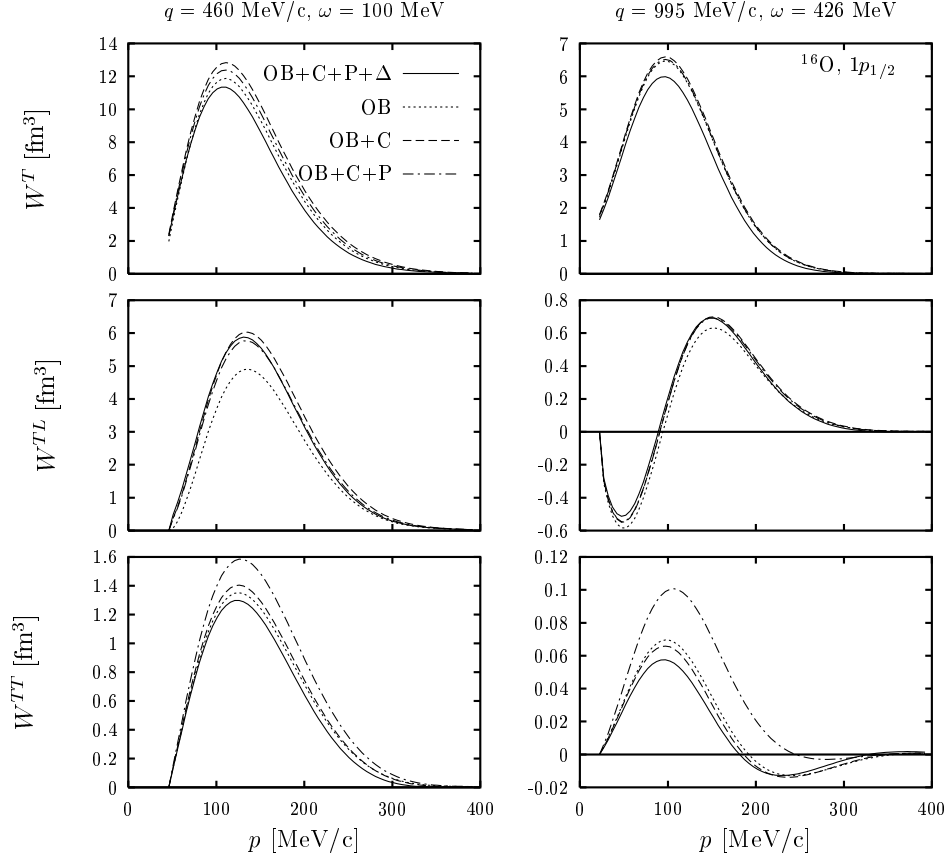


Figure 7: Separate contribution of each one of the MEC to the exclusive response functions. SR results are shown for knock-out from the  $1p_{1/2}$  shell of  $^{16}\text{O}$  for the same kinematics as in fig. 6, including the one-body current only (OB), and in addition the contact (C), pionic (P) and  $\Delta$  currents in the calculation.

between the spin-orbit term and the magnetization current gives rise to a contribution in  $W^{TL}$  which is of the same order of magnitude as the interference between the charge density and convection current. Thus the presence of the spin-orbit term in the density is essential to describe properly the response  $W^{TL}$ , even for moderate  $q$ -values.

Analogous results hold for a proton knockout from the  $p_{3/2}$ -shell in  $^{16}\text{O}$ : the role of relativity in each response is similar to the one observed for the  $p_{1/2}$  case and, again, the most sensitive response to relativistic effects is  $W^{TL}$ . However, the relativistic enhancement for the  $p_{3/2}$ -orbit is somewhat smaller than the one presented for  $p_{1/2}$ , particularly for large  $q$ .

The separate contributions of the MEC is presented in figs. 7 and 8 for  $p_{1/2}$  and  $p_{3/2}$ -shells, respectively. Kinematics is as in the previous figure and we do not show results for the pure longitudinal response as it is not affected by MEC within the present approaches. We compare the OB responses (dotted line) with the results obtained when including the contact (C) current (dashed line), the contact and pion-in-flight (C+P) currents (dot-dashed line),

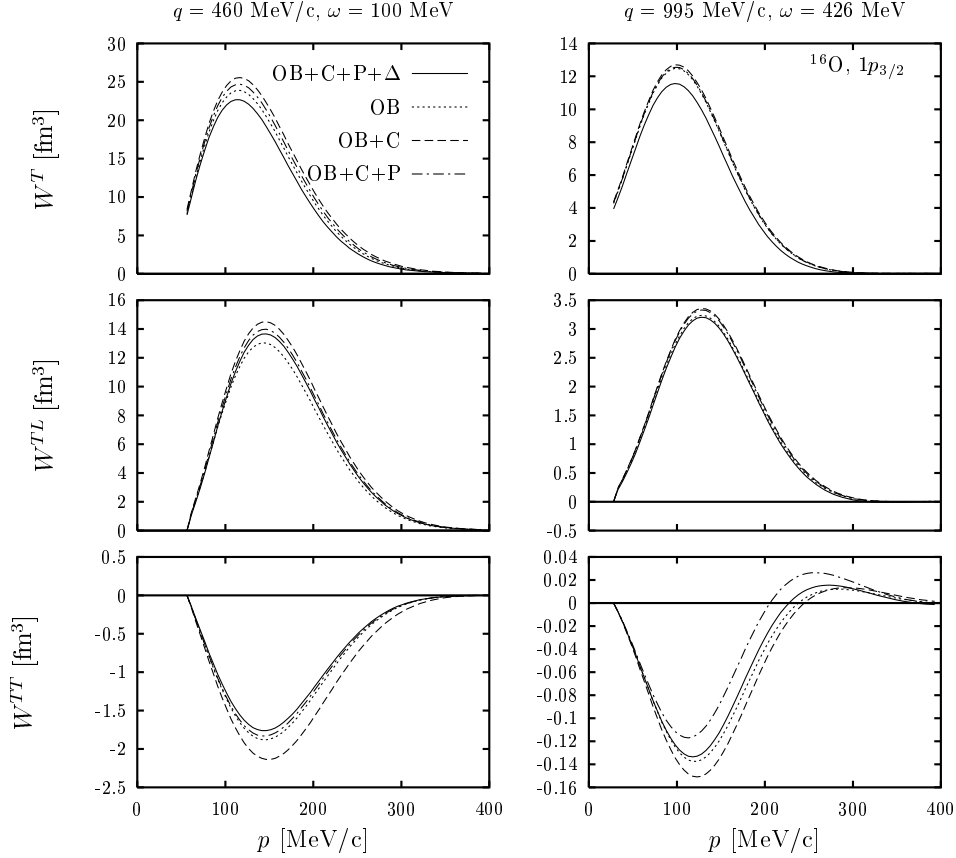


Figure 8: The same as fig. 7 for knock-out from the  $1p_{3/2}$  shell of  $^{16}\text{O}$ .

and the contact, pionic and  $\Delta$  (C+P+ $\Delta$ ) currents (solid line). Let us analyze each response separately. In the case of  $W^T$ , the contact current produces an increase which is partially cancelled by the tiny reduction introduced by the pionic current. Note that the role of the C and P currents is negligible for large  $q$ . The  $\Delta$  current gives rise to an additional reduction whose relative magnitude is rather similar for both shells. The total effect of C+P+ $\Delta$  MEC is a reduction of the T response which is slightly more important for high  $q$ .

Although a great caution should be taken in extending the conclusions drawn from the analysis of exclusive reactions to inclusive ones or viceversa, it is illustrative to discuss the results relative to quasielastic ( $e, e'p$ ) reactions in connection with the quasielastic ( $e, e'$ ) ones. Note that, apart from the potentials usually considered in both types of reactions, the inclusive responses are calculated by integrating the exclusive ones over the ejected nucleon variables, and summing over all occupied hole states, i.e., including also the contribution given by the  $1s_{1/2}$  shell. In refs. [31, 37, 38] we evaluated the role of MEC for the inclusive  $T$  response in a relativistic Fermi gas model. The contact (C) contribution was found to be larger than the pion-in-flight term (P), a dominance increasing with  $q$ . The total (C+P) contribution presents an oscillatory behaviour with respect to the transferred energy  $\omega$ , having a node close to the QEP value, particularly for high  $q$ . For  $q = 1$  GeV/c, this node

is reached for  $\omega \sim 435$  MeV, which is very close to the value  $\omega = 426$  MeV selected in the  $(e, e'p)$  calculations (right hand panels in figs. 7 and 8). On the contrary, in the case  $q = 500$  MeV/c, the contribution of the C+P currents in the inclusive  $T$  response presents a node for  $\omega \sim 150$  MeV and is positive and non-negligible for the value  $\omega = 100$  MeV selected here in the case of  $(e, e'p)$  process. A similar discussion can be also applied to the  $\Delta$  results. In ref. [38] (see also previous section) the  $\Delta$  contribution to the inclusive  $T$  response has been shown to be always negative up to  $q \sim 2$  GeV/c and larger than the one provided by the C and P currents together. Hence the general trend of the MEC contribution to the inclusive channel agrees with the effects shown for the exclusive responses (figs. 7 and 8).

Finally, comparing the results in figs. 7 and 8 we conclude that the effects of MEC for the exclusive  $T$ -response are similar for both  $p_{1/2}$  and  $p_{3/2}$  shells. A different behaviour is found in the results of ref. [25] where the role of MEC, for  $q = 460$  MeV/, is shown to be larger in the case of the  $p_{3/2}$  shell. In addition, the role introduced by the pionic current (P) in [25] is said to be negligible, whereas in our case its contribution, though a little bit smaller than the contact term, is clearly visible. Our results are also in disagreement with the calculation of [21] performed for  $q = 1$  GeV, where the total MEC effect is found to be small for the  $p_{1/2}$  and large for the  $p_{3/2}$  in the  $T$  response. This discrepancy is linked to the FW method used to implement relativity in [21] which is not expected to be applicable for  $q = 1$  GeV [37].

Next we focus on the interference  $TL$  response. From figs. 7 and 8 we observe that for  $q = 460$  MeV/c the MEC effect is larger in the case of the  $p_{1/2}$ -shell. The main contribution comes from the contact current, which produces an enhancement in  $W^{TL}$  of the order of  $\sim 20\%$  for  $p_{1/2}$  and  $\sim 15\%$  for  $p_{3/2}$ , while the role of the pion-in-flight is smaller, reducing the response, and in particular, the  $\Delta$  gives rise to an almost negligible contribution (slightly positive for  $p_{1/2}$  and negative for  $p_{3/2}$ ). These results disagree with the findings of ref. [25], where the effect of the  $\Delta$  in  $W^{TL}$  is substantially large and negative for the  $p_{1/2}$ -shell, so that it cancels out the contact term, yielding a negligible global MEC contribution. On the contrary, in the same reference the  $\Delta$  contribution for the  $p_{3/2}$ -orbit is found to be large and positive, hence the net effect of MEC is an important enhancement in the  $TL$  response. As in the case of the pure  $T$  response, the pionic contribution found in [25] is negligible, which again is not in accord with our results.

Figs. 7 and 8 clearly show that the importance of the MEC on the  $TL$  response decreases as  $q$  goes to higher values. Whereas the contact current enhances the  $TL$  response by the same magnitude for the two  $p$ -shells, the  $\Delta$  term is negligible for the  $p_{1/2}$  and tends to cancel the contact contribution for  $p_{3/2}$ . For both shells, the pionic current does not alter  $W^{TL}$ .

As far as  $W^{TT}$  is concerned, note that this response is much smaller, its contribution being of order  $(k_F/m_N)^2$  (see ref. [32]); hence terms of second order in  $p/m_N$ , usually neglected in the expansion of the current operators, may provide a crucial role in this response. However, since  $W^{TT}$  is also particularly sensitive to the details of the model, it can be used as a test to compare different theoretical models. Note that this response is opposite in sign for  $p_{1/2}$  and  $p_{3/2}$ . Concerning the role of MEC, it is found to be of the same relative order of magnitude as in the other responses, except for the pionic current which has an important effect in this case.

As a further application of our model we present in fig. 9 the  $TL$  asymmetry ( $A_{TL}$ ) for  $p_{1/2}$

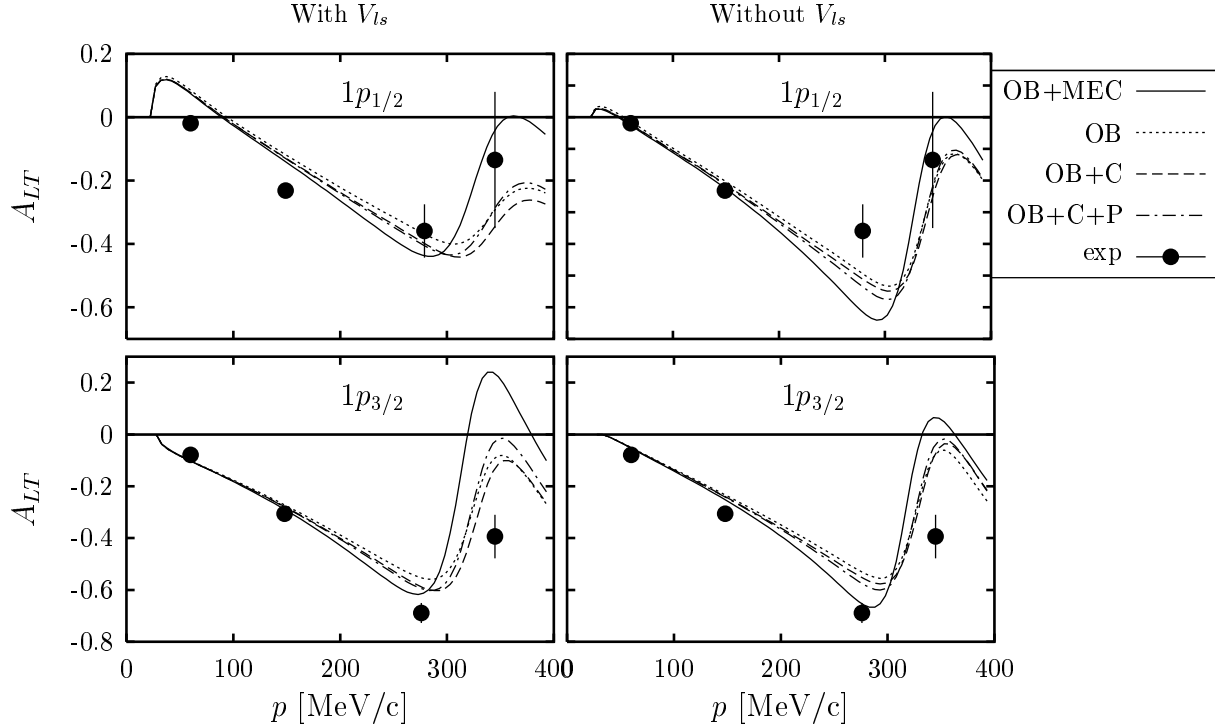


Figure 9:  $A_{TL}$ -asymmetry for proton knock-out from the  $1p_{1/2}$  and  $1p_{3/2}$  shells in  $^{16}\text{O}$ , computed within the SR model including the successive contribution of each one of the MEC. Experimental data are from [8]. Left and right panels have been obtained to including or not the spin orbit part in the optical potential.

(top panels) and  $p_{3/2}$  (bottom panels). The kinematics has been selected to correspond to the experimental data [8].  $A_{TL}$  is obtained from the difference of cross sections measured at  $\phi' = 0^\circ$  and  $\phi' = 180^\circ$  divided by the sum, hence this observable is particularly interesting because it does not depend on the spectroscopic factors. A detailed study on the  $TL$  asymmetry has been carried out in refs. [6, 7] within the relativistic distorted-wave impulse approximation (RDWIA), namely a fully relativistic calculation without including MEC. In particular, a comparison between  $A_{TL}$  evaluated in RDWIA and using the SR approach for the one-body current and neglecting MEC, was presented in [6]. There it was proved the large contribution given by the spin-orbit correction to the charge density, and, more importantly, the crucial role played by the dynamical enhancement of the lower components of bound Dirac spinors in the description of interference  $TL$  observables (see also refs. [47, 48]). Recent data on polarization observables nicely agree with RDWIA analysis [49, 50].

However, a direct calculation of the role of MEC in  $A_{TL}$  within a relativistic approach has never been performed, as far as we know. Thus, in fig. 9 we show the results obtained within the impulse approximation, i.e., without MEC (dotted line), and the contributions introduced by the various two-body currents: C (dashed line), C+P (dot-dashed line) and total MEC, namely C+P+ $\Delta$  (solid line). In order to investigate also the dependence of our

results on the FSI, in fig. 9 we show two sets of calculations for each  $p$  shell: including the spin-orbit part of the optical potential  $V_{ls}$  [46] (left panels) and without it (right panels). For comparison we also present the experimental data [8]. From inspection of fig. 9 we conclude that the effect of MEC is very small for low missing momentum values and it starts to be important for  $p \geq 300$  MeV/c. Note however that in this region the dynamical enhancement of lower components, obviously not considered within the present SR approach, starts also to play a crucial role and hence it should be considered before a detailed comparison with data can be accomplished. Note also the large discrepancy between the SR calculation and the data for low  $p$  in the case of  $p_{1/2}$  with the full potential. This issue was already present in [6], where the RDWIA calculation differs from the SR one comparing better with data [8]. This problem within the SR approach appears to be connected with the spin-orbit term introduced by the equivalent Schrödinger form of the optical potential, as can be seen in the right panels of fig. 9, that do not include  $V_{ls}$  in the FSI. Our results also show that the MEC effects for high missing momenta strongly depend upon the FSI, since they are substantially reduced when only the central part of the optical potential is included (right panels).

Summarizing, from theoretical results in fig. 9 and ref. [6], and their comparison to experimental data [8], we may conclude the following: i) a fully relativistic calculation within the impulse approximation (RDWIA), i.e., including the effects introduced by the dynamical enhancement of the lower components in the Dirac spinors, appears to be essential to reproduce the data; ii) the effects introduced by MEC for high missing momentum values seem to be also very important, and highly dependent on the FSI. Hence an appropriate relativistic analysis of these two-body currents may be also essential in order to improve the description of the experimental data at high missing momentum.

## 4 Conclusions

In this paper we have presented a semi-relativistic model of inclusive and exclusive electron scattering from nuclei in the one-nucleon emission channel, including one- and two-body currents. These currents differ from the usual non-relativistic ones by multiplicative  $(q, \omega)$ -depending factors obtained by an expansion in powers of the missing momentum. An essential ingredient of the SR consists in using, in addition to the SR currents, relativistic kinematics to relate the energy and momentum of the ejected nucleon.

This model has been already tested in quasielastic inclusive  $(e, e')$  processes in refs. [31, 37, 38]. In this paper we have first focussed on the new SR- $\Delta$  current and compared its contribution to the inclusive transverse response with a fully relativistic calculation in RFG for moderate and high  $q$ -values. This has allowed us to test the reliability of different prescriptions introduced to account for “dynamical” aspects of the  $\Delta$  propagator. We have found that the best agreement with the fully relativistic calculation corresponds to the static limit approximation. Thus, we conclude that the use of any of these “dynamized”  $\Delta$  propagators within the one-particle emission channel is not justified and, moreover, it may produce very large discrepancies with the exact result.

Next we have implemented the SR currents into a DWIA model of the quasielastic  $(e, e'p)$  reaction, computing the separate response functions and the  $TL$  asymmetry, using the static

limit for the  $\Delta$  propagator. After analyzing the role of the different relativistic corrections embedded in our calculation and its dependence upon the momentum transfer, we have studied the effect of MEC on the different observables. In particular, we have compared the results for proton knock-out from the  $p_{1/2}$  and  $p_{3/2}$  shells in  $^{16}\text{O}$ , choosing quasi-perpendicular kinematics, typical of the experiments. In the case of the  $T$  response, MEC effects are shown to be equally important for the two shells, giving rise to a net reduction of the response. For  $W^{TL}$ , the role of MEC is to enhance the response, an effect that is substantially larger for the  $p_{1/2}$  shell, and reduces considerably for high  $q$ -values. In general, we get sizable differences with previous calculations in the literature [21, 25].

Finally, our model applied to the  $A_{TL}$  asymmetry shows that this observable is very sensitive to the MEC and to FSI in the region of high missing momentum. Since it has been proved in [6] that the interference  $TL$  observables, particularly  $A_{TL}$ , are also crucially affected by other relativistic ingredients, such as the dynamical enhancement of lower components, not included in this work, it would be very interesting to evaluate MEC effects within the scheme of the fully relativistic calculation of refs. [4, 6, 7], and contrast their predictions with the ones obtained with the present SR model.

## Acknowledgments

This work was partially supported by funds provided by DGI (Spain) and FEDER funds, under Contracts Nos BFM2002-03218 and BFM2002-03315 and by the Junta de Andalucía and by the INFN-CICYT exchange. M.B.B. acknowledges financial support from MEC (Spain) for a sabbatical stay at University of Sevilla (ref. SAB2001-0025).

## References

- [1] S. Boffi, C. Giusti, F.D. Pacati, Phys. Repts. **226** (1993) 1.
- [2] S. Boffi, C. Giusti, F.D. Pacati, M. Radici, *Electromagnetic response of atomic nuclei*. Clarendon Press, Oxford, 1996.
- [3] J.J. Kelly, Adv. Nucl. Phys. **23** (1996) 75.
- [4] J.M. Udías, P. Sarriguren, E. Moya de Guerra, E. Garrido, J.A. Caballero, Phys. Rev. **C48** (1993) 2731; **C51** (1995) 3246.
- [5] J.M. Udías, P. Sarriguren, E. Moya de Guerra, J.A. Caballero, Phys. Rev. **C53** (1996) R1488.
- [6] J.M. Udías, J.A. Caballero, E. Moya de Guerra, J.E. Amaro, T.W. Donnelly, Phys. Rev. Lett. **83** (1999) 5451.
- [7] J.M. Udías, J.A. Caballero, E. Moya de Guerra, J.R. Vignote, A. Escuderos, Phys. Rev. **C64** (2001) 024614.

- [8] J. Gao *et al.*, Phys. Rev. Lett. **84** (2000) 3265.
- [9] D. Van Neck, M. Waroquier, A.E.L. Dieperink, S.C. Pieper, V.R. Pandharipande, Phys. Rev. **C57** (1998) 2308.
- [10] M. Mazziotta, J.E. Amaro, F. Arias de Saavedra, Phys. Rev. **C65** (2002) 034602.
- [11] I. Bobeldijk *et al.*, Phys. Rev. Lett. **73** (1994) 2684.
- [12] H. Mütter, A. Polls, Prog. Part. Nucl. Phys. **45** (2000) 243.
- [13] A. Fabrocini, G. Co', Phys. Rev. **C63** (2001) 044319.
- [14] C. Mahaux, R. Sartor, Adv. Nucl. Phys. **20** (1991) 1.
- [15] Z.Y. Ma, J. Wambach, Phys. Lett. **B256** (1991) 1.
- [16] A. Fabrocini, Phys. Rev. **C55** (1997) 338.
- [17] J.E. Amaro, G. Co', A.M. Lallena Nucl. Phys. **A578** (1994) 365.
- [18] S. Boffi, M. Radici, Nucl. Phys. **A526** (1991) 602.
- [19] V. Van der Sluys, J. Ryckebusch, M. Waroquier, Phys. Rev. **C49** (1994) 2695.
- [20] J.E. Amaro, A.M. Lallena, J.A. Caballero, Phys. Rev. **C60** (1999) 014602.
- [21] J. Ryckebusch, D. Debruyne, W. Van Nespen, S. Janssen, Phys. Rev. **C60** (1999) 034604.
- [22] J. Ryckebusch, Phys. Rev. **C64** (2001) 044606
- [23] D.O. Riska, in *Mesons in Nuclei, Vol. II*, M. Rho and D.H. Wilkinson, Eds., North-Holland Publishing Co., (1979).
- [24] J.E. Amaro, A.M. Lallena, G. Co', Ann. Phys. **221** (1993) 306.
- [25] C. Giusti, F.D. Pacati, nucl-th/0211007
- [26] T. Wilbois, P. Wilhelm, H. Arenhövel, Phys. Rev. **C54** (1996) 3311
- [27] J. Ryckebusch, L. Machenil, M. Vanderhaeghen, V. Van der Sluys, M. Waroquier, Phys. Rev. **C54** (1996) 3313
- [28] P. Wilhelm, H. Arenhovel, C. Giusti, P.D. Pacati, Z. Phys. **A359** (1997) 467.
- [29] A. Meucci, C. Giusti, F.D. Pacati, Phys. Rev. **C66** (2002) 034610.
- [30] J.E. Amaro, J.A. Caballero, T.W. Donnelly, E. Moya de Guerra, A.M. Lallena, J.M. Udías, Nucl. Phys. **A602** (1996) 263.

- [31] J.E. Amaro, M.B. Barbaro, J.A. Caballero, T.W. Donnelly, A. Molinari, Phys. Rep. **368** (2002) 317.
- [32] J.E. Amaro, J.A. Caballero, T.W. Donnelly, E. Moya de Guerra, Nucl. Phys. **A611** (1996) 163.
- [33] J.E. Amaro, T.W. Donnelly, Ann. Phys. **263** (1998) 56.
- [34] J.E. Amaro, T.W. Donnelly, Nucl. Phys. **A646** (1999) 187.
- [35] J.E. Amaro, T.W. Donnelly, Nucl. Phys. **A703** (2002) 541.
- [36] J.E. Amaro, M.B. Barbaro, J.A. Caballero, T.W. Donnelly, A. Molinari, Nucl. Phys. **A643** (1998) 349
- [37] J.E. Amaro, M.B. Barbaro, J.A. Caballero, T.W. Donnelly, A. Molinari, Nucl. Phys. **A697** (2002) 451.
- [38] J.E. Amaro, M.B. Barbaro, J.A. Caballero, T.W. Donnelly, A. Molinari, nucl-th/0301023, submitted to Nucl. Phys. A.
- [39] J.W. Van Orden, T.W. Donnelly, Ann. Phys. **131** (1981) 451.
- [40] W.M. Alberico, T. W. Donnelly, A. Molinari, Nucl. Phys. **A512** (1990) 541.
- [41] W.M. Alberico, M.B. Barbaro, A. De Pace, T.W. Donnelly, A Molinari, Nucl. Phys. **A563** (1993) 605.
- [42] J. Nieves, E. Oset, C. Garcia Recio, Nucl. Phys. **A554** (1993) 554.
- [43] J. Nieves, E. Oset, C. Garcia Recio, Nucl. Phys. **A554** (1993) 509.
- [44] A.S. Raskin, T.W. Donnelly, Ann. Phys. **191** (1989) 78.
- [45] J.R. Comfort, B. C. Karp, Phys. Rev. **C21** (1980) 2162.
- [46] E.D. Cooper, S. Hama, B.C. Clark, R.L. Mercer, Phys. Rev. **C47** (1993) 297.
- [47] J.A. Caballero, T.W. Donnelly, E. Moya de Guerra, J.M. Udías, Nucl. Phys. **A632** (1998) 323; **A643** (1998) 189.
- [48] M.C. Martínez, J.A. Caballero, T.W. Donnelly, Nucl. Phys. **A707** (2002) 83; **A707** (2002) 121.
- [49] R.J. Woo *et. al.*, Phys. Rev. Lett. **80** (1998) 456.
- [50] J.M. Udías, J.R. Vignote, Phys. Rev. **C62** (2000) 034302.